

NT@UW-01-07

Exploring Skewed Parton Distributions with Two-body Models on the Light Front I: bimodality

B. C. Tiburzi and G. A. Miller
 Department of Physics
 University of Washington
 Box 351560
 Seattle, WA 98195 – 1560

June 14, 2019

Abstract

We explore skewed parton distributions for simple, model wave-functions in a truncated two-body Fock space. Consideration of non-Gaussian wave functions is our main emphasis, from which we observe the distributions are bimodal (there can be two distinct peaks) in the Fock-space diagonal overlap region ($x > \xi$). We demonstrate that this behavior arises from convoluting two light-front wave functions to form the skewed parton distribution. Furthermore, the factorization *Ansätze*, which have been used often, are shown not to hold. At high t , we can write the skewed parton distribution in terms of quark distribution amplitudes and perturbative wave functions thereby providing new tests.

1 Introduction

Recently there has been considerable interest in the connection between hard inclusive and exclusive reactions, which has been, in part, due to the unifying rôle of skewed parton distributions (SPD's) [1, 2, 3]. Aside from being the natural marriage of form factors and parton distributions, SPD's appear when one tries to calculate hadronic matrix elements such as in Compton scattering [3, 4, 5], and the electroproduction of mesons [6, 7].

There is much effort underway related to the measurement of these functions [8]. Intuitively clear, but simple models [3, 9, 10, 11] have been used to provide first calculations (and more sophisticated approaches have been pursued [12, 13]). In this paper, we attempt to gain intuition about the structure of these distributions, using simple light-front wave functions. We find a new feature, bimodality (or double peaks), which is rather general and thus independent of sophisticated formalism. To this end, we work only with simple, two-body, model wave-functions for scalar particles and express the SPD as a convolution of these light-front wave-functions. This is, of course, a (very) specific instance of the general light-cone Fock-space expansion of the SPD's carried out in [14]. Of crucial importance is the employment of non-Gaussian wave-functions. As we shall show, the bimodal nature of SPD's is absent for Gaussian wave-functions. We remark that the bimodality of these distributions has been encountered before in [12] where the authors study the SPD's in the chiral quark-soliton model of the nucleon. There it was shown that contributions from discrete levels and the Dirac continuum interfere, resulting in a roughly bimodal

quark distribution (for $x > \xi$). We show below that there exists a rather general explanation for the bimodal behavior in terms of light-front wave-functions.

We review the definition and kinematics of the SPD in section 2 and proceed to the two-body Fock space in section 3. Once in section 4, we present the wave-functions used and then provide a visual array of SPD's illustrating their functional behavior. Finally we conclude briefly in section 5.

2 Definitions and kinematics

The skewed parton distribution is a non-diagonal matrix element of bilocal field operators. Various conventions, reference frames, variables, *etc.* exist for the description of such an object. Below we adopt the conventions of the *off-forward* parton distribution of Ji [15]. This choice is natural for a symmetric treatment of initial and final hadron states and consequently time-reversal invariance will be manifest.

We shall consider the SPD for a toy scalar "meson" of mass M consisting of two scalar "quarks", each of mass m . Such a model restricts the SPD to only one kinematical régime (one that is diagonal in Fock-space). This restriction in modeling SPD's was encountered from the start [10], and we take up the issue of extending model SPD's to all kinematical régimes in [16].

Let us parameterize the kinematics as follows. The initial meson momentum is denoted by $P^\mu = (P^-, P^+, \mathbf{P}^\perp)$, with $P^\pm = (P^0 \pm P^3)/\sqrt{2}$, and the final meson momentum is denoted P'^μ . The average momentum between initial and final states is thus $\bar{P}^\mu = (P^\mu + P'^\mu)/2$. Defining $x \bar{P}^+$ to be the momentum conjugate to light-front distance y^- , we have [17]

$$F(x, \xi, t) = \frac{i \bar{P}^+}{2(P^+ + P'^+)} \int \frac{dy^-}{2\pi} e^{iy^- x \bar{P}^+} \langle P' | \hat{\phi}^\dagger(-y^-/2) \partial^+ \hat{\phi}(y^-/2) - \partial^+ \hat{\phi}^\dagger(-y^-/2) \hat{\phi}(y^-/2) | P \rangle, \quad (1)$$

where the skewness ξ is defined by $\xi = -\Delta^+ / 2 \bar{P}^+$ with Δ as the momentum transfer suffered by the meson, namely $\Delta^\mu = P'^\mu - P^\mu$, with $P'_\perp = -P_\perp = \Delta_\perp/2$, and the invariant $t \equiv \Delta^2$. As spelled out in [15], time-reversal invariance forces $F(x, \xi, t) = F(x, -\xi, t)$. It is easy to see why this must be the case in Eq. (1) owing to the reality of F and the Hermiticity of the current operator. Without any loss of generality, we take $\xi > 0$ below. Notice the form of the above equation is such that when integrated over all x , we recover the electromagnetic form factor (calculated from the + component of the current operator).

Having set forth all kinematical variables, we must then use Lorentz invariance to derive any remaining relations among them. Since our final meson is still intact, $P^2 = P'^2 = M^2$ and thus $\bar{P}^2 = M^2 - t/4$. Exploiting $\Delta \cdot \bar{P} = 0$, we find $\Delta^- = \xi \bar{P}^2 / \bar{P}^+$, and also an expression for the transverse momentum transfer

$$\Delta^{\perp 2} = -4\xi^2 M^2 - t(1 - \xi^2). \quad (2)$$

This implies a maximal skewness $\xi_m = 1/\sqrt{1 - 4M^2/t}$ for a given t .

In order to unearth the physics hidden in Eq. (1), we insert the mode expansion [18] of the scalar field operators:

$$\hat{\phi}(y^-, \mathbf{y}^\perp) = \int \frac{d\mathbf{k}^+ d\mathbf{k}^\perp}{\sqrt{2\mathbf{k}^+(2\pi)^3}} \theta(\mathbf{k}^+) \hat{a}(\mathbf{k}^+, \mathbf{k}^\perp) e^{-i(y^- \mathbf{k}^+ - \mathbf{y}^\perp \cdot \mathbf{k}^\perp)}, \quad (3)$$

with the quark creation and annihilation operators satisfying the relation

$$[\hat{a}(k^+, \mathbf{k}^\perp), \hat{a}^\dagger(\kappa^+, \kappa^\perp)] = (2\pi)^3 \delta(k^+ - \kappa^+) \delta^2(\mathbf{k}^\perp - \kappa^\perp). \quad (4)$$

Evaluating the plus-derivative of the field operators and inserting this along with the mode expansion Eq. (3) into the expression for the SPD, we find

$$F(x, \xi, t) = \frac{1}{4} \int \frac{d k^+ d \mathbf{k}^\perp}{\sqrt{2 k^+} (2\pi)^3} \frac{d \kappa^+ d \kappa^\perp}{\sqrt{2 \kappa^+} (2\pi)^3} \theta(k^+) \theta(\kappa^+) \delta(x \bar{P}^+ - \frac{k^+ + \kappa^+}{2}) (k^+ + \kappa^+) \langle P' | \hat{a}^\dagger(\kappa^+, \kappa^\perp) \hat{a}(k^+, \mathbf{k}^\perp) | P \rangle. \quad (5)$$

3 Two-body, truncated Fock space

We now proceed with representing the SPD as a convolution of light-front wave functions. In order to do so, we must write the meson states as sums of their light-front Fock-space components. The light-front Fock-space is the ideal arena in which to decompose hadronic states [19, 20], since, apart from zero-modes, the perturbative vacuum is trivial. In this formalism, physical matrix elements are then expressed as a sum of Fock-space component overlaps (in general these overlaps are non-diagonal in particle number). The general form of the SPD written in terms of N -body Fock space components was carried out in Ref. [14] and is a natural choice for these distributions since, e.g. the positivity constraints [21] are automatically satisfied [10]. Since one has little knowledge concerning viable N -body light-front wavefunctions, this formalism is limited to the lower Fock-space components. In order to gain initial intuition about the SPD's, we shall limit ourselves to the two-body sector.

With a truly empty perturbative light-front vacuum $\hat{a}|0\rangle = 0$, we can build our quark states from the vacuum in the usual fashion

$$|k\rangle \equiv |q; k^+, \mathbf{k}^\perp\rangle = \hat{a}^\dagger(k^+, \mathbf{k}^\perp) |0\rangle. \quad (6)$$

We shall keep the Fock-space as small as possible by truncating at quark pairs. In this approximation, our meson states appear as

$$|P\rangle = \sqrt{2 P^+} (2\pi)^3 \int \left(\prod_{j=1}^2 \frac{d p_j^+ d \mathbf{p}_j^\perp}{\sqrt{2 p_j^+} (2\pi)^3} \right) \delta^{2,+}(P - p_1 - p_2) \Psi(p_1, p_2) |p_1, p_2\rangle. \quad (7)$$

Several points must be clarified about the above expression. We are using shorthand notation for light-front momenta. Upper-case letters refer to meson momenta, while quark momenta are denoted by lower-case. The components $(+, \perp)$ are now implicit and we have notationally condensed the three-dimensional light-front delta function into $\delta^{2,+}$.

The light-front wave function Ψ appears in Eq. 7. The remarkable property of light-front wave functions is that they depend only on the relative momenta of their constituents, not on the hadron's momentum [22]. Our two-body wave function is only a function of the plus-momentum fraction x , and the relative transverse momentum \mathbf{p}^\perp , namely

$$\Psi(p_1, p_2) = \sqrt{2(p_1^+ + p_2^+)} \psi\left(x = \frac{p_1^+}{p_1^+ + p_2^+}, \mathbf{p}^\perp = (1-x)\mathbf{p}_1^\perp - x\mathbf{p}_2^\perp\right) \quad (8)$$

$\Psi(p_1, p_2)$ is a symmetric function of p_1 and p_2 . We also choose the normalization

$$\int \frac{dx d\mathbf{k}^\perp}{2(2\pi)^3 x(1-x)} |\psi(x, \mathbf{k}^\perp)|^2 = 1. \quad (9)$$

It is worthwhile to state the normalization of the state $| P \rangle$. The use of Eqs. (4,6) gives

$$\langle P_3, P_4 | p_1, p_2 \rangle = (2\pi)^6 (\delta^{2,+}(p_1 - p_3)\delta^{2,+}(p_2 - p_4) + \{1 \leftrightarrow 2\}) \quad (10)$$

Thus we have

$$\langle P' | P \rangle = P^+ \delta^{2,+}(P' - P) \int \frac{d^{2,+}p_1 d^{2,+}p_2}{p_1^+ p_2^+} \delta^{2,+}(P - p_1 - p_2) |\Psi(p_1, p_2)|^2 \quad (11)$$

At this point, we must separate out the meson's momentum by defining total and relative momentum variables: $\mathcal{P} = p_1 + p_2$ with $(+, \perp)$ understood, $x = p_1^+ / P^+$ and $\mathbf{p}^\perp = (1-x) \mathbf{p}_1^\perp - x \mathbf{p}_2^\perp$. The variable differentials are related by $d^{2,+}p_1 d^{2,+}p_2 = \frac{P^+}{2} d^{2,+}\mathcal{P} dx d\mathbf{p}^\perp$. Carrying out the change of variables allows us to perform the integral over $d^{2,+}\mathcal{P}$ trivially since now the delta function $\delta^{2,+}(P - \mathcal{P})$ sits in the integrand. The remaining integral is over relative coordinates and is merely the wave function's normalization

$$\begin{aligned} \langle P' | P \rangle &= P^+ \delta^{2,+}(P' - P) \int \frac{dx d\mathbf{p}^\perp}{x(1-x)} |\psi(x, \mathbf{p}^\perp)|^2 \\ &= 2 P^+ (2\pi)^3 \delta^{2,+}(P' - P). \end{aligned} \quad (12)$$

To evaluate the SPD, we insert the two-body expansion (7) into equation (5) and calculate the matrix element

$$\langle P' | \hat{a}^\dagger(\kappa^+, \kappa^\perp) \hat{a}(\mathbf{k}^+, \mathbf{k}^\perp) | P \rangle = 2\sqrt{P^+ P'^+} (2\pi)^3 \frac{\delta^{2,+}(P' - P + k - \kappa) \Psi(P - k, k) \Psi^*(\kappa, P' - \kappa)}{\sqrt{\mathbf{k}^+ \kappa^+ (P^+ - \mathbf{k}^+) (P'^+ - \kappa^+)}} \quad (13)$$

Using the delta function to perform the integral $d^{2,+}\kappa$ yields

$$\begin{aligned} F(x, \xi, t) &= \sqrt{P^+ P'^+} \int \frac{d^{2,+}k (2\mathbf{k}^+ + \Delta^+) \theta(x - \xi)}{8(2\pi)^3 \mathbf{k}^+ (P^+ - \mathbf{k}^+) (\mathbf{k}^+ - 2\xi P^+)} \delta((x + \xi) \bar{P}^+ - k^+) \Psi(P - k, k) \Psi^*(k + \Delta, P - k) \\ &= \frac{x(1 - \xi^2) \theta(x - \xi)}{2(2\pi)^3 (1-x)(x^2 - \xi^2)} \int d\mathbf{k}^\perp \psi^* \left(\frac{x - \xi}{1 - \xi}, \mathbf{k}^\perp + \frac{1 - x}{1 - \xi^2} \Delta^\perp \right) \psi \left(\frac{x + \xi}{1 + \xi}, \mathbf{k}^\perp \right), \end{aligned} \quad (14)$$

where we see the result of the theta functions present in Eq. (5) is to restrict the value of x : $1 > x > \xi$.

The above result is consistent with the time-reversal invariance of our starting expression Eq. (1) since it is clearly even in ξ . In the forward limit ($t = 0$), we recover the toy model quark distribution function

$$F(x, 0, 0) = \int \frac{d\mathbf{k}^\perp}{2(2\pi)^3 x(1-x)} |\psi(x, \mathbf{k}^\perp)|^2 \equiv q(x). \quad (15)$$

Finally in the case of zero skewness we should arrive at the electromagnetic form-factor (after having integrated over x) [3]. We find

$$\int dx F(x, 0, t) = \int \frac{dx d\mathbf{k}^\perp}{2(2\pi)^3 x(1-x)} \psi(x, \mathbf{k}^\perp) \psi^*(x, \mathbf{k}^\perp + (1-x)\Delta^\perp) \equiv F(t), \quad (16)$$

which is indeed the Drell-Yan formula [23]. As pointed out in Ref. [10], the restriction to one kinematical régime ($x > \xi$) does not allow for the sum rule to be verified—Eq. (16) is as much as we can hope for now. We shall take up the issue of verifying the sum rule in Ref. [16].

Note that the form of the SPD does not support various factorization *Ansätze*[24]. For example, in the limit $\xi \rightarrow 0$, $F(x, \xi, t) \neq q(x)F(t)$, though this *Ansatz* does satisfy the sum rule. Such a factorized form only holds for Gaussian wave functions when $\xi = 0$. Counting the number of field operators in equation 1, we see there is no physical basis for such a factorized *Ansatz* when $\xi = 0$.

4 Model wave functions

It remains only to choose two-body light-front wave functions to explore the SPD derived in Eq. (14). Before we do so, it is wise to review the existing literature on modeling SPD's. Radyushkin investigated them for a scalar toy model [3] deriving analytical results. They were investigated for a bag model of the nucleon in [9], in the chiral quark-soliton model [12] and in 1 + 1 dimensional QCD [13]. More in line with our above analysis, SPD's were modeled using light-front Fock-space components in [10] (using N -body Gaussian wave functions for low values of N), for the pion using a Gaussian wave function in [11], and for the QED electron in [25].

We will use three different wave functions to contrast the behavior of the SPD: a Gaussian (G), the Hulthén wave function (H) of Ref. [26], and the (weak-binding) Wick-Cutkosky wave function (WC) of Ref. [27]. Each wave function contains a normalization constant N , which is determined from the normalization condition used above in Eq. (9).

Our Gaussian wave function is taken to be

$$\psi_G(x, \mathbf{k}^\perp) = \frac{\sqrt{Nf(x)}}{m} e^{-\frac{\mathbf{k}^\perp 2 + m^2}{\mu^2 x(1-x)}}, \quad (17)$$

where $f(x) = x^{0.3}(1-x)^{2.25}\sqrt{1+6x}$ is similar to a valence quark distribution (the difference from the quark distribution of Eq.(15) is due to the mass term in the exponential). We choose $\frac{m}{\mu} = 1$ and $\frac{M}{\mu} = 1.8$.

The Hulthén wave function has the form

$$\psi_H(x, \mathbf{k}^\perp) = \frac{m\sqrt{N}x(1-x)}{4x(1-x)\alpha^2 + (2x-1)^2m^2 + \mathbf{k}^\perp 2} (\delta_a^\alpha - \delta_b^\alpha), \quad (18)$$

with $\frac{a}{m}, \frac{b}{m}$ chosen to be the phenomenological deuteron parameters.

Lastly the Wick-Cutkosky wave function in the weak-binding limit is

$$\psi_{WC}(x, \mathbf{k}^\perp) = \frac{m^3\sqrt{N}x^2(1-x)^2}{(4x(1-x)\kappa^2 + (2x-1)^2m^2 + \mathbf{k}^\perp 2)^2} \frac{1}{1 + |2x-1|}, \quad (19)$$

with $\kappa = \frac{1}{2}ma$, the meson mass $M = 2m - \frac{1}{4}ma^2$. We choose a suitably weak coupling of $a = 0.08$. The form of the wave function is basically Coulombic with a multiplicative retardation term.

In Figure 1 we contrast the quark distribution function for each of the toy models under consideration. The models clearly differ in how narrowly the quark distribution is peaked. The Wick-Cutkosky distribution appears sharply peaked at $x = 1/2$ which is characteristic of a weakly bound system.

Next in Figure 2, we use our Gaussian wave function ψ_G in Eq. (14) to reproduce a typical Gaussian SPD found in the literature. We note the distribution maintains its characteristic Gaussian shape as a function of ξ . The peak of the distribution, however, appears to be suppressed as ξ increases up to ξ_m . Since (as we will show) the special form of the Gaussian wave function obscures the general structure of the SPD, we proceed to consider the power-law wave functions.

Let us plot the SPD using Eq. (14) for the Wick-Cutkosky wave function ψ_{WC} . In Figure 3, we show the $\xi = 0.07$ slice of the SPD at $-t/m^2 = 0.1$. The distribution is bimodal, with the two peaks displaced from $x = 1/2$. To understand this feature, we crank up the momentum transfer to $-t/m^2 = 100$. The larger momentum transfer allows us to probe a larger skewness (since ξ_m increases with $-t$). At this higher momentum transfer, let us look at another ξ -slice of the SPD as a function of x shown in Figure 4.

Perhaps the bimodal nature of the distribution is not too surprising, after all the SPD is a convolution of two hadronic wave functions. The weak binding Wick-Cutkosky wave function is by nature highly peaked at $x = 1/2$.

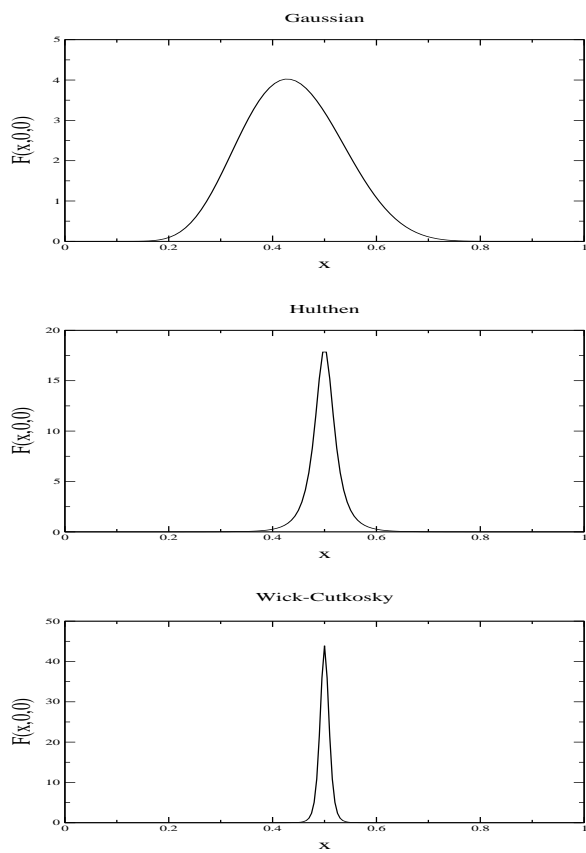


Figure 1: Quark distribution functions $F(x, 0, 0)$ plotted versus x for the models under consideration.

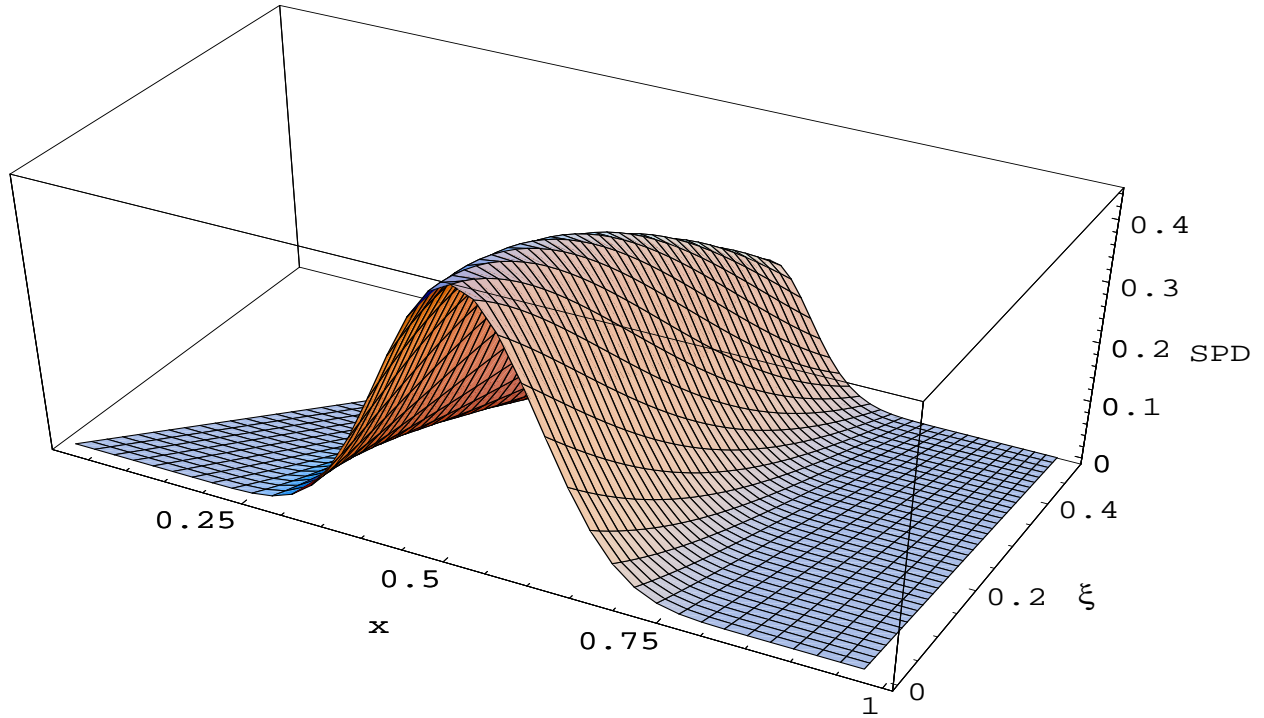


Figure 2: Skewed parton distribution for 2-body Gaussian model using the parameters: $m/\mu = 1, M/\mu = 1.8$ and evaluated for $-t/M^2 = 1.23$.

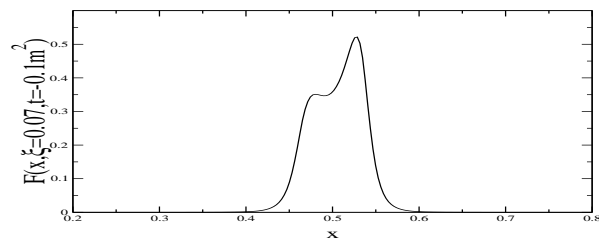


Figure 3: Bimodality encountered in the Wick-Cutkosky Model's skewed parton distribution. The SPD is plotted as a function of x for $-t/m^2 = 0.1$ and $\xi = 0.07$.

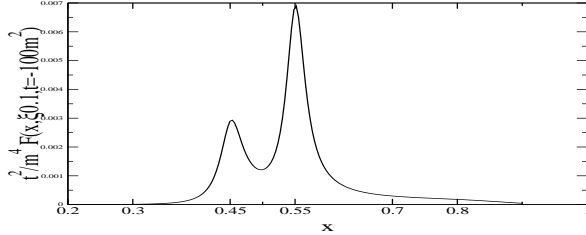


Figure 4: Bimodality in the Wick-Cutkosky Model's skewed parton distribution at high momentum transfer. The SPD is plotted as a function of x for $-t/m^2 = 100$ and $\xi = 0.1$.

The integration over the transverse momentum \mathbf{k}^\perp in Eq. (14) does not affect the location of the peak. Due to the convoluted nature of the SPD, the x location of the wave function's peak becomes a function of ξ . Let us denote the location of ψ 's peak— $\psi(\alpha(x, \xi), \mathbf{k}^\perp)$ with the arguments in Eq. (14)—as $x_p(\xi)$ and that of ψ^* by $\bar{x}_p(\xi)$. Using Eq. (14), we find

$$\begin{aligned} x_p(\xi) &= \frac{1}{2}(1 - \xi) \\ \bar{x}_p(\xi) &= \frac{1}{2}(1 + \xi). \end{aligned}$$

Thus for fixed t , as the skewness ξ is increased, the peaks of ψ and ψ^* trek in opposite directions. For $\xi = 0.1$, the peak of ψ should be located at $x_p = 0.45$ and that of ψ^* at $\bar{x}_p = 0.55$. Looking back at Figure 4 shows us this is indeed the case. This allows us to understand the peaks' behavior for the full range of ξ shown in Figure 5, where we see a ripple which heads to smaller x as ξ increases. Once $\xi > 1/3$ we can be assured the SPD's peak is due to ψ^* . But the figure opens up new questions. What can we say about the height of the peaks?

Looking at all the SPD's displayed so far for the Wick-Cutkosky model, generally the peaks at lower x which stem from ψ aren't quite the lofty summits as those from ψ^* which are at higher x . This asymmetry is due to the prefactor in the SPD: $\frac{x(1-\xi^2)}{(1-x)(x^2-\xi^2)}$ which generally increases with increasing x for fixed values of ξ . Thus the peaks due to ψ^* are preferentially enhanced while those due to ψ tend to be flattened as they trek to lower x .

Taking a second glance at Figure 5, we see another feature of these distributions. The peak which we attribute to ψ^* is amplified with increasing ξ . To be able to make definite statements, we take the asymptotic limit and appropriately analyze the SPD. (We will find that this leads to generally true qualitative information for lower momentum transfer.) The Wick-Cutkosky wave function has power-law dependence, and so we appeal to the approach of Brodsky and Lepage [19] of approximating integrals over \mathbf{k}^\perp using the knowledge that our wave functions are peaked for low values of \mathbf{k}^\perp . Looking at Eq. (14) and taking Δ^\perp very large compared to \mathbf{k}^\perp , we realize the dominant contributions come from either $\mathbf{k}^\perp \approx 0$ or $\mathbf{k}^\perp \approx -\frac{1-x}{1-\xi^2}\Delta^\perp$ for which one of the wave functions is greatly suppressed. This gives:

$$F(x, \xi, t/m^2 \gg 1) \approx \frac{x(1-\xi^2)}{2(2\pi)^3(1-x)(x^2-\xi^2)} \left(\phi(x_1)\psi^*(x_2, (1-\bar{x})\Delta^\perp) + \phi^*(x_2)\psi(x_1, -(1-\bar{x})\Delta^\perp) \right), \quad (20)$$

where $\phi(x) = \int d\mathbf{k}^\perp \psi(x, \mathbf{k}^\perp)$ and we've abbreviated the plus-momentum fraction arguments as $x_1 = \frac{x+\xi}{1+\xi}$, $x_2 = \frac{x-\xi}{1-\xi}$ and their average $\bar{x} = (x_1 + x_2)/2$. Notice that the above equation reproduces the correct location of the peaks as a function of x . The Wick-Cutkosky wave function, as well as the Hulthén behave as $\psi \sim 1/t^2$ for large $|t|$. In a realistic calculation, one would use wave functions calculated from perturbative Quantum Chromodynamics (pQCD). These wave functions have different asymptotic behavior ($\psi_{\text{pQCD}} \sim 1/t$) than our model wave functions since the dynamics of pQCD stems from vector exchange (unlike the scalar exchange implicitly employed by our models).

Using the form of Eq. (20), we can deduce whether the wave functions are being stressed by increasing ξ . The wave functions will be stressed depending on whether larger transverse momentum flows through them as ξ increases. Thus we are concerned as to whether $(1 - \bar{x})\Delta^\perp$ increases with ξ (for fixed t and x). Taking the derivative with respect to ξ shows that the change in transversal momentum flow depends upon the sign of $|t|(1 - \xi^2) - (1 + \xi^2)4M^2$. Hence, if $|t|/4M^2 < 1$, then less momentum will flow through the wave functions as ξ increases. Otherwise, there is initially increasing momentum flow (starting from $\xi = 0$) followed by decreasing momentum flow with ξ [28]. In either case, as ξ approaches its maximum value (the maximal skewness ξ_m), there is less transverse momentum flowing through the wave functions in Eq. (20) and consequently the height of the summit (centered at \bar{x}_p) will increase.

This fact is evidenced by Figure 5. Given the log-scale, we see the SPD increases by a factor ~ 10 near maximal skewness. To quantitatively understand this rise in the distribution, we'd be wise to consider the transverse momentum flowing through the wave functions. The ratio of the transverse momentum flow (in asymptopia) to the mass is given by $\delta(\xi) = (1 - \bar{x})|\Delta^\perp|/M$. For fixed x (say near the peak of ψ^* as we go to maximal skewness) and fixed t , we can plot this ratio as a function of ξ which is done in Figure 6. Indeed near maximal skewness, there is a drop ($\sim 10\times$) in δ and consequently we expect a rapid rise in the distribution since (rather suddenly) the wave functions aren't as stressed.

The arguments presented above have been general for power-law wave functions and so aptly apply to the Hulthén model wave function as well. We can find the SPD's for the Hulthén model by inserting ψ_H into equation 14. At the moderate momentum transfer of 1 GeV^2 the bimodality is visible in the $\xi = 0.15$ slice of the SPD, see Figure 7. The peaks are not quite so distinct since the Hulthén wave function isn't as narrowly peaked about $x = 1/2$ compared to the Wick-Cutkosky. Consequently distinguishability between contributions from ψ and ψ^* diminishes. As we go to higher momentum transfer, the trends become as clear as before. Figure 8 plots the SPD at $|t| = 20 \text{ GeV}^2$ which matches up to the Wick-Cutkosky SPD (Figure 5) in every detail. At 20 GeV^2 , the maximal skewness is $\xi_m \approx 0.77$. In the plot, we have shown the full range of ξ . The bimodality is still visible for $\xi < 1/3$ but the scale is dominated by the rise toward maximal skewness. We ran into this in the Wick-Cutkosky model (and was the reason we previously used the logarithmic scale in Figure 5). Taking our focus away from the bimodal peaks, we see the distribution rises ($\sim 5\times$) as ξ approaches maximal skewness even against the competing prefactor $1 - \xi^2$. The power-law Hulthén wave function is clearly recovering from being stressed as we approach maximal skewness.

Finally we must remark, the altered view of Figure 8 not only allows us to view the bimodality more clearly, it also hides a feature of in our model wave function! If we could look into the large x shadows in Figure 8, we would notice a striking asymmetry present even at $\xi = 0$. The cross section shown in Figure 9 highlights this feature. This built-in asymmetry persists in the SPD for $\xi \neq 0$ [29]. Recall that the SPD at $\xi = 0$ gives the un- x -integrated electromagnetic form factor. In light of our previous work with the Hulthén model form factor [26], we readily interpret the asymmetry as due to factorization breaking present in this model. The dominant contribution to the electromagnetic form factor in asymptopia comes from a peak in the near end-point region ($x \lesssim 1$) and dominates the contribution from the peak at $x = 1/2$ by a factor of $\ln |t|$. As $|t|$ is increased the asymmetry shown in Figure 9 will develop into a strong peak in the near end-point region giving rise to the logarithmic modification to the form factor.

Of course logarithmic, asymptotic modifications to the form factor are also present for the Wick-Cutkosky model [30]. One finds a near end-point asymmetry for the Wick-Cutkosky SPD as well, however, due to the value of model

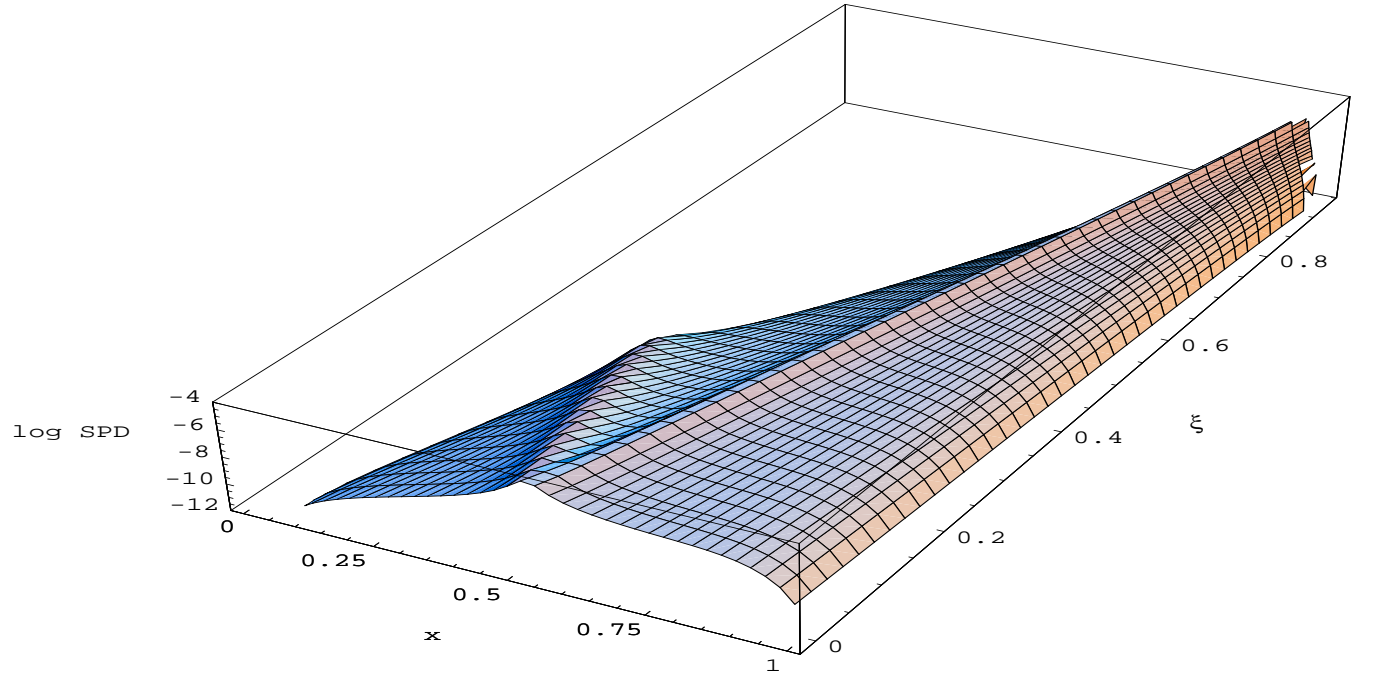


Figure 5: Skewed parton distribution for Wick-Cutkosky Model, with the model parameter $a = 0.08$, evaluated for $-t/m^2 = 100$. This asymptotic momentum transfer allows us to see and understand the general features of the distribution. Notice we plot the logarithm of the SPD.

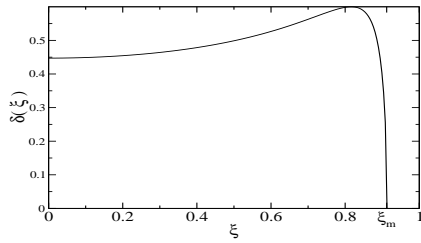


Figure 6: Ratio of transverse momentum flow to M : $\delta(\xi) = (1 - \bar{x})|\Delta^\perp|/M$, plotted as a function of ξ (taken here for $t/M = -20$ and $x = 0.9$). Note the drastic drop as we approach maximal skewness.

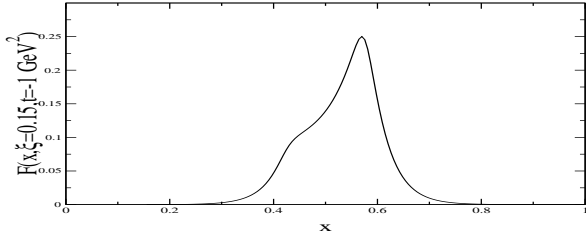


Figure 7: Hulthén SPD for $|t| = 1 \text{ GeV}^2$ and $\xi = 0.15$ illustrating the bimodality.

parameter chosen ($a = 0.08$), one must go to considerably high momentum transfer ($|t|/m^2 \sim 10^5$) to see this effect.

Having visited the power-law, model wave functions, we must come full circle. What about the Gaussian wave function we initially considered? We must remark that the logic leading to Eq. (20) depends crucially on the fact that the wave functions have power-law momentum dependence. Thus arguments about transversely stressed wave functions simply do not apply and we cannot gain intuition about the SPD's amplitude. Moreover (owing to the peculiar nature of Gaussians) taking the convolution of two Gaussian wave functions yields another Gaussian wave function (certainly with a different *effective* plus-momentum, but a Gaussian nonetheless). Thus bimodality (which was due to the individual nature of ψ and ψ^*) disappears. Moreover, at large momentum transfer, we do not see an amplification of the SPD near maximal skewness. On the contrary, the Gaussian SPD's are suppressed. Indeed the behavior of Gaussian wave functions is peculiar (not just due to unimodality). Luckily we have a wealth of intuition about power-law wave functions and thus our understanding of the structure of skewed parton distributions need not remain cloudy. The amplification (with ξ) of the SPD is a possible signature for power-law dependence. Physical observables (the deeply virtual Compton scattering cross section, for example) depend on weighted x -integrals of the SPD. Thus maximal skewness amplification could be canceled by compensating behavior in the other kinematical regimes.

5 Concluding remarks

Above we have derived the form of the skewed parton distribution in terms of two-body light-front wave functions in the region $x > \xi$. We then used model wave functions in order to explore the resulting distributions and gain intuition about their structure. The key results are: Eq. (14), that the use of power-law wave functions leads to skewed parton distributions with two peaks, that factorization of $F(x, \xi = 0, t)$ of into separate functions of x and t does not hold, and finally Eq.(20). This last item gives $F(x, \xi, t)$ for very large values of t in terms of quark distribution amplitudes and perturbative wave functions. Thus SPD's give a new way to investigate perturbative treatments.

Acknowledgment

This work was funded by the U. S. Department of Energy, grant: DE-FG03 – 97ER41014.

References

[1] D. Muller, D. Robaschik, B. Geyer, F. M. Dittes and J. Horejsi, Fortsch. Phys. **42**, 101 (1994) [hep-ph/9812448].

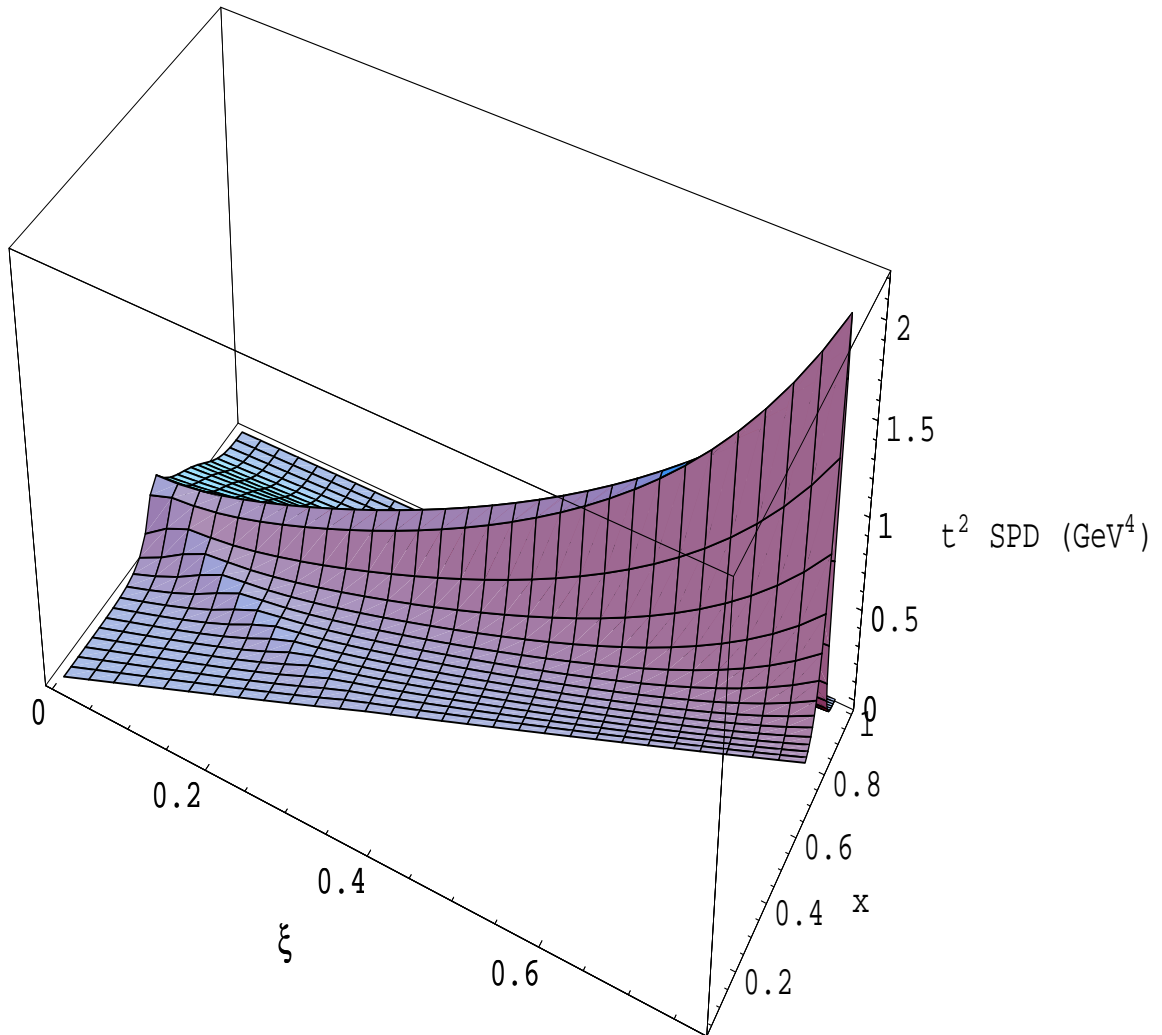


Figure 8: Skewed parton distribution for the Hulthén model plotted for $|t| = 20 \text{ GeV}^2$. The trends at this high momentum transfer are now identical to those in the Wick-Cutkosky model.

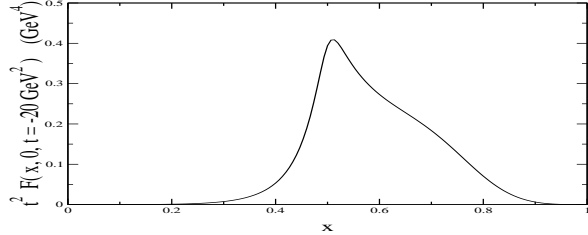


Figure 9: Un- x -integrated Hulthén form factor for $|t| = 20 \text{ GeV}^2$, i.e. the SPD evaluated for $\xi = 0$. The factorization violating peak has already started to develop (manifesting itself as an asymmetry).

- [2] X. Ji, Phys. Rev. Lett. **78**, 610 (1997); Phys. Rev. D **55**, 7114 (1997)
- [3] A. V. Radyushkin, Phys. Rev. D **56**, 5524 (1997)
- [4] X. Ji and J. Osborne, Phys. Rev. D **58**, 094018 (1998)
- [5] J. C. Collins and A. Freund, Phys. Rev. D **59**, 074009 (1999)
- [6] A. V. Radyushkin, Phys. Lett. B **385**, 333 (1996)
- [7] J. C. Collins, L. Frankfurt and M. Strikman, Phys. Rev. D **56**, 2982 (1997)
- [8] M. Guidal and M. Vanderhaeghen, hep-ph/9901298.
- [9] X. Ji, W. Melnitchouk and X. Song, Phys. Rev. D **56**, 5511 (1997)
- [10] M. Diehl, T. Feldmann, R. Jakob and P. Kroll, Eur. Phys. J. C **8**, 409 (1999)
- [11] H. Choi, C. Ji and L. S. Kisslinger, hep-ph/0104117.
- [12] V. Y. Petrov, P. V. Pobylitsa, M. V. Polyakov, I. Bornig, K. Goeke and C. Weiss, Phys. Rev. D **57**, 4325 (1998)
- [13] M. Burkardt, Phys. Rev. D **62**, 094003 (2000)
- [14] M. Diehl, T. Feldmann, R. Jakob and P. Kroll, Nucl. Phys. B **596**, 33 (2001)
- [15] X. Ji, J. Phys. **GG24**, 1181 (1998)
- [16] B. C. Tiburzi, G. A. Miller, *Exploring Skewed Parton Distributions with Two-body Models on the Light-front II: covariant Bethe-Salpeter approach*, in preparation.
- [17] Our expression for the SPD tacitly employs the light-front gauge in which $A^+ = 0$.
- [18] Since our Fock-space expansion will be truncated to just quark pairs, the results will not depend on whether we retain anti-particles in the mode expansion. This is done to eliminate from the start kinematical régimes not under consideration.

- [19] S. J. Brodsky and G. P. Lepage, SLAC-PUB-4947 *IN *MUELLER, A.H. (ED.): PERTURBATIVE QUANTUM CHROMODYNAMICS* 93-240 AND SLAC STANFORD - SLAC-PUB-4947 (89,REC.JUL.) 149p.*
- [20] S. J. Brodsky, hep-ph/0102051.
- [21] B. Pire, J. Soffer and O. Teryaev, Eur. Phys. J. C **8**, 103 (1999)
- [22] P. A. Dirac, Rev. Mod. Phys. **21**, 392 (1949); H. Leutwyler and J. Stern, Annals Phys. **112**, 94 (1978).
- [23] S. D. Drell and T. Yan, Phys. Rev. Lett. **24**, 181 (1970); G. B. West, Phys. Rev. Lett. **24**, 1206 (1970).
- [24] M. Vanderhaeghen, P. A. Guichon and M. Guidal, Phys. Rev. Lett. **80** (1998) 5064; Phys. Rev. D **60**, 094017 (1999).
- [25] S. J. Brodsky, M. Diehl and D. S. Hwang, Nucl. Phys. B **596**, 99 (2001)
- [26] B. C. Tiburzi and G. A. Miller, Phys. Rev. C **63**, 044014 (2001)
- [27] V. A. Karmanov, Nucl. Phys. B **166**, 378 (1980).
- [28] One can show that where the derivative vanishes (ξ_0) always occurs before the maximal skewness, *vis.* $\xi_0 < \xi_m$. Thus one is always guaranteed that less transversal momentum will flow through the wave functions for *physical* ξ which are large enough.
- [29] The factorization violating peak in the near end point region is actually reduced as ξ increases. Since the peak comes from logarithmic modifications present for this model in asymptopia, we must reason that for lower transverse momentum flow the violation will be less. But this is precisely what happens as we increase ξ —less transversal momentum flows through the wave functions due to the ξ dependence of Δ^\perp . This is why the asymmetry is not visible from our vantage point (maximal ξ) in the high x shadows in Figure 8. That means factorization breaking present in these models has nothing to do with the great amplification of the SPD as we approach maximal skewness (*cf.* Figure 5 where no factorization breaking is visible but maximal skewness amplification certainly occurs).
- [30] V. A. Karmanov and A. V. Smirnov, Nucl. Phys. A **546**, 691 (1992).